Applied and Environmental Microbiology, July 2008, p. 4491–4497 Vol. 74, No. 14
0099-2240/08/$08.00+0 doi:10.1128/AEM.00255-08

Listeria monocytogenes EGD-e Biofilms: No Mushrooms but a Network of Knitted Chains▽

Aurélie Rieu,[4] Romain Briandet,[3] Olivier Habimana,[3] Dominique Garmyn,[1,2] Jean Guzzo,[4] and Pascal Piveteau[1,2]*

Université de Bourgogne, UMR 1229, F-21000 Dijon, France[1]; INRA, UMR 1229, F-21000 Dijon, France[2]; UMR 763, Unité Mixte de Recherche en Bioadhesion et Hygiène des Matériaux, INRA-AgroParisTech, F-91300 Massy, France[3]; and Laboratoire de Recherche En Vigne et Vin, Université de Bourgogne, IUVV, F-21000 Dijon, France[4]

Received 29 January 2008/Accepted 13 May 2008

Listeria monocytogenes **is a food pathogen that can attach on most of the surfaces encountered in the food industry. Biofilms are three-dimensional microbial structures that facilitate the persistence of pathogens on surfaces, their resistance toward antimicrobials, and the final contamination of processed goods. So far, little is known about the structural dynamics of *L. monocytogenes* biofilm formation and its regulation. The aims of this study were, by combining genetics and time-lapse laser-scanning confocal microscopy (LSCM), (i) to characterize the structural dynamics of *L. monocytogenes* EGD-e sessile growth in two nutritional environments (with or without a nutrient flow), and (ii) to evaluate the possible role of the *L. monocytogenes agr* system during biofilm formation by tracking the spatiotemporal fluorescence expression of a green fluorescent protein (GFP) reporter system. In the absence of nutrient flow (static conditions), unstructured biofilms composed of a few layers of cells that covered the substratum were observed. In contrast, when grown under dynamic conditions, *L. monocytogenes* EGD-e biofilms were highly organized. Indeed, ball-shaped microcolonies were surrounded by a network of knitted chains. The spatiotemporal tracking of fluorescence emitted by the GFP reporter system revealed that *agr* expression was barely detectable under static conditions, but it progressively increased during 40 h under dynamic conditions. Moreover, spatial analysis revealed that *agr* was expressed preferentially in cells located outside the microcolonies. Finally, the in-frame deletion of *agrA*, which encodes a transcriptional regulator, resulted in a decrease in initial adherence without affecting the subsequent biofilm development.**

Biofilms are communities of microorganisms attached to a surface (44). Several steps can be identified during biofilm development. After an initial step of reversible, then irreversible, adherence, bacteria grow as microcolonies and spread on the surface; also, biofilms develop as complex, three-dimensional (3D) structures during the maturation step (17). The microorganisms undergo profound changes during their transition from planktonic cells (free-floating organisms) to cells that are part of a complex, surface-attached community (sessile organisms) (44), and cells develop an increased resistance to antimicrobial agents (34, 38, 64). For this reason, the removal of established biofilms requires harsh treatments, with most using oxidizing biocides (18, 20, 25, 54). The presence of biofilms raises safety issues in the food industry, especially when biofilms are located on food-processing surfaces and pipelines that are unreachable by washing agents (8). Clearly, biofilms can become a health hazard by harboring pathogenic bacteria such as *Listeria monocytogenes* (4). Moreover, *L. monocytogenes* is capable of attaching and developing biofilms on a variety of surfaces, such as stainless steel, polymers, and rubber gaskets (2, 3, 13, 36, 40). *L. monocytogenes* is a gram-positive human pathogen that is responsible for serious infections among immunocompromised individuals and pregnant women (19).

Several systems to study biofilms have been used to identify and characterize the bacterial elements and genetic determinants involved in biofilm development. For instance, plate counting has been used to quantify sessile cells of *L. monocytogenes* on abiotic surfaces (1, 5–7, 10, 12, 13, 32, 43, 47, 52, 53). Also, biofilms of *L. monocytogenes* have been quantified by using the microplate adhesion method (3, 11, 23, 33, 48), while their structures have been investigated by scanning electron microscopy (SEM) (3, 12, 13, 28, 32, 39, 49), epifluorescence microscopy (9, 24, 28, 36, 37, 41, 46), or laser-scanning confocal microscopy (LSCM) (10, 31, 51). LSCM has allowed the visualization of fully hydrated samples and has revealed the elaborate 3D structure of biofilms (14). The generally accepted structure of *Pseudomonas aeruginosa* biofilm is composed of mushroom-shaped microcolonies, in which cells are embedded in an exopolymeric cement and the microcolonies are separated by channels and voids (29, 58). Reports concerning the structure of *L. monocytogenes* biofilm are available. Few studies have used LSCM to investigate the structure of *L. monocytogenes* biofilm (10, 31, 51).

Biofilm development and maturation requires complex cellular mechanisms in which cell-cell communication is involved. Among these, the *agr* system plays a role during the biofilm development of *Staphylococcus aureus* (61, 65), *Enterococcus faecalis* (22), and *Lactobacillus plantarum* (57) and during the early stages of the biofilm formation of *L. monocytogenes* (48). Indeed, the deletion of the gene coding for the response regulator AgrA impaired the ability of *L. monocytogenes* EGD-e to adhere to abiotic surfaces (48).

To characterize the biofilm development of *L. monocytogenes*, several models of growth, media, and bacterial strains

* Corresponding author. Mailing address: Laboratoire de Microbiologie du Sol et de l'Environnement UMR UB/INRA 1229, 17 Rue de Sully, BP86510, F-21065 Dijon, France. Phone: 33 3 80 69 34 32. Fax: 33 3 80 69 32 24. E-mail: piveteau@u-bourgogne.fr.

▽ Published ahead of print on 23 May 2008.

TABLE 1. Bacterial strains, plasmids, and oligonucleotides used in this study

Bacterial strain, plasmid, or oligonucleotide	Relevant property(ies)[a]	Created restriction site	Reference or source
Bacteria			
E. coli TOP10	Cloning host		Invitrogen
L. monocytogenes EGD-e	Wild type of serotype 1/2a, for which the genome sequence is available		42
L. monocytogenes DG125A	EGD-e with in-frame deletion of *agrA* gene		48
L. monocytogenes AR009	Em^r, Cm^r derivative of EGD-e harboring pGID128 in integrative form		This work
L. monocytogenes AR011	Em^r, Cm^r derivative of DG125A harboring pGID128 in integrative form		This work
Plasmids			
pGF-EM	Em^r, Cm^r, Am^r; 9.4-kb derivative of pCON-1 carrying 0.8-kb *gfp* gene of pKV111 and *erm* gene of Tn*917*		35
pGID113	Km^r Am^r, 4.7-kb derivative of pCRII-TOPO carrying 0.7-kb P*agr* region promoter		This work
pGID120	Em^r,Cm^r, Am^r; 10.4-kb derivative of pGF-EM carrying 0.6-kb P*agr* region promoter inserted into HindIII/XbaI site of pGID113		This work
pGID128	Em^r, Cm^r, Am^r; derivative of pGID120 carrying the P*agr-gfp* translational fusion obtained after restriction by XbaI/NheI		This work
Primers (5′→3′)[b]			
AGRB5	TGAGCTATGAAGACGCGATT		
AGRB6	A**TCTAGA**CAACTAATTCACCTCCACTA	XbaI	

[a] Em^r, erythromycin resistant; Cm^r, chloramphenicol resistant; Km^r, kanamycin resistant; and Am^r, ampicillin resistant.
[b] Specific restriction sites are underlined, and extra nucleotides added to include restriction sites in the PCR product are shown in boldface.

from the literature were used, and the influence of several environmental parameters were assessed. For example, the temperature of incubation affects *L. monocytogenes* biofilm growth (7, 52, 53). In the present study, we investigated the kinetics of *L. monocytogenes* EGD-e development in biofilms by LSCM under two different environmental conditions; i.e., static and flowing systems. Second, we determined the *agr* expression in situ during biofilm development by using the green fluorescent protein (GFP) reporter.

MATERIALS AND METHODS

Bacterial strains, plasmids, and culture conditions. The bacterial strains and plasmids used in this study and their characteristics are shown in Table 1. *L. monocytogenes* was cultivated in tryptic soy broth (TSB; Biokar Diagnostics, Pantin, France) at 25°C for biofilm and planktonic cultures and in brain heart infusion broth (BHI; Biokar Diagnostics) at 40°C for strain construction. *Escherichia coli* TOP10 (Invitrogen, Cergy Pontoise, France) cells were grown aerobically in Luria-Bertani broth (Biokar Diagnostics) at 37°C. When appropriate, antibiotics (Sigma, St. Quentin Fallavier, France) were added as follows: kanamycin, 50 $\mu g \cdot ml^{-1}$ (for *E. coli*); ampicillin, 200 $\mu g \cdot ml^{-1}$ (for *E. coli*); chloramphenicol, 10 $\mu g \cdot ml^{-1}$ or 7.5 $\mu g \cdot ml^{-1}$ (for *L. monocytogenes*) (Table 1).

Strain and plasmid construction. The reporter plasmid pGID128 contains a fusion of the *agr* promoter region (located 690 bp upstream of the start codon) with *gfp*, the gene coding for GFP. First, the *agr* promoter region was amplified by PCR with primers AGRB5 and AGRB6 (Invitrogen) (Table 1) and *Taq* DNA polymerase (Q-Biogene, MP Biomedicals, Illkirch, France) using *L. monocytogenes* EGD-e genomic DNA as a template. This PCR product was cloned into the pCRII-TOPO vector (Invitrogen) to obtain pGID113, and this vector was transferred into chemically competent *E. coli* TOP10 cells as recommended by the manufacturer (Invitrogen). Second, plasmid pGID113 was digested with HindIII/XbaI (Invitrogen), and the resulting 617-bp fragment containing the promoter region of the *agr* operon (P*agr*) was ligated into pGF-EM (35) that had been restricted with HindIII/XbaI (Invitrogen) to obtain pGID120. Third, this pGID120 plasmid was digested with XbaI/NheI (Invitrogen) to obtain pGID128. The strains EGD-e and DG125A (Δ*agrA*) (48) were transformed by pGID128, and the transformants were selected on BHI agar plates (Biokar diagnostics) containing 10 $\mu g \cdot ml^{-1}$ chloramphenicol. These strains were named AR009 and AR011 (Δ*agrA*), respectively, and harbored plasmid pGID128 in the integrative form.

Biofilm growth conditions. (i) Static biofilm experiments. AISI 304 stainless steel chips (25 by 25 by 1 mm; Goodfellow SARL, Lille, France) were inserted in separate 55-mm-diameter petri dishes (Dominique Dutscher S.A., Brumath, France) that contained 8 ml of TSB. Chloramphenicol (7.5 $\mu g \cdot ml^{-1}$) was added to the growth medium to ensure the stable carriage of plasmid pGID128. An overnight culture of strains AR009 and AR011 (Δ*agrA*) in TSB at 25°C was used to inoculate (1/100, vol/vol) TSB in petri dishes, which were incubated at 25°C. The medium was removed after 2 h, and then every 24 h fresh TSB (8 ml) was added. Cell adhesion and biofilm development were evaluated by microscopic observations after 2, 24, and 48 h at 25°C. Following incubation, the medium was removed and 8 ml of saline solution (150 mM NaCl) was gently poured onto the chips to remove loosely adhering bacteria. Sessile cells were stained with a 0.01% SYTO61 (Molecular Probes, Invitrogen) solution. This stain penetrates and stains nucleic acids in both live and dead cells. Three independent experiments were performed.

(ii) Flow-cell biofilm experiments. Biofilms were cultivated in flow cell BST FC 81 (Biosurface Technologies Corporation, Bozeman, MT), with channel dimensions of 1.6 by 12.7 by 47.5 mm. The flow cells are small continuous-flow systems with a glass viewing port that allows the direct observation of the biofilms without disrupting the community. Flow chambers were inoculated with overnight cultures of the AR009 and AR011 (Δ*agrA*) strains in TSB medium (1/100, vol/vol). After inoculation, the medium flow was stopped for 1 h to allow bacterial adhesion, and thereafter the medium was pumped through the flow cells at 10 ml/h by using a peristaltic pump (model 205S; Watson Marlow, Falmouth, England, United Kingdom). Flow-cell biofilms were stained with the nucleic acid stain SYTO61 (http://probes.invitrogen.com/lit/catalog/3/sections/2426.html) after 16, 24, and 40 h of incubation at 25°C before microscopic observations. Two independent experiments with two replicates each were made.

LSCM and image processing. Image acquisition was performed on a Leica TCS SP2 AOBS (Leica Microsystems, France) laser-scanning confocal laser microscope on the MIMA2 microscopic platform (http://voxel.jouy.inra.fr/mima2). LSCM allowed the simultaneous 3D monitoring of GFP and SYTO61 dyes. The excitation wavelength used for GFP was 488 nm, and the emitted fluorescence was collected in the range of 500 to 600 nm. The red fluorescent nucleic acid stain SYTO61 was excited at 633 nm, and the emitted fluorescence was collected in the range of 650 to 700 nm. Images were collected through a ×63 Leica oil immersion objective (numeric aperture, 1.4). Simulated 3D fluorescence projections and vertical cross-sections through the biofilms were generated

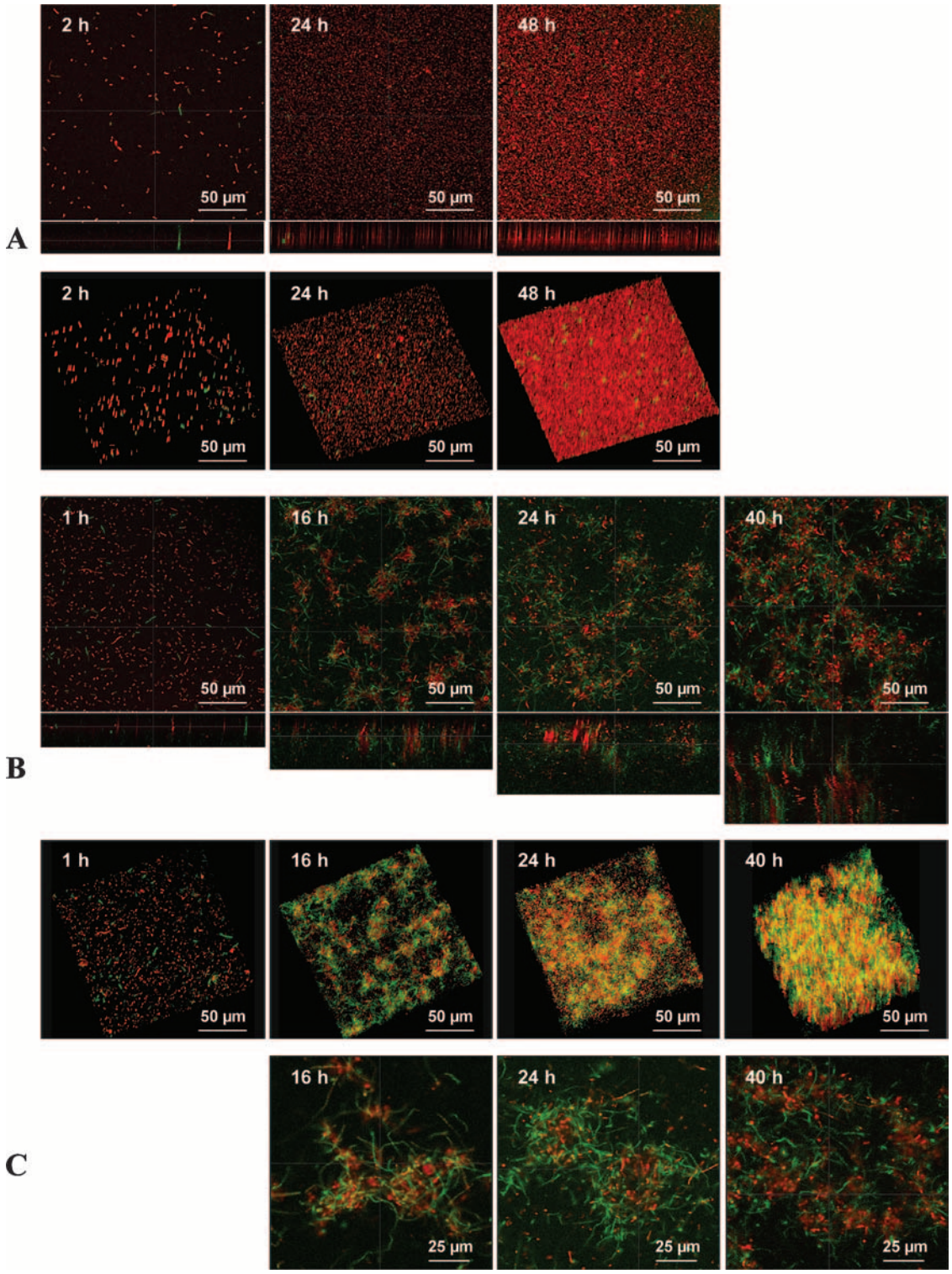

FIG. 1. Scanning confocal micrographs (upper lines) and 3D reconstruction of a z stack (lower lines) of biofilms formed by *L. monocytogenes* AR009 in TSB medium at 25°C under static conditions after 2, 24, and 48 h of incubation (A) and under flowing conditions after 1, 16, 24, and 40 h of incubation (B). (C) Biofilms grown under flowing conditions and observed at a higher magnification. Green indicates those cells expressing GFP from the reporter plasmid pGID128, which contains a fusion of the *agr* promoter region with *gfp*. The red cells are stained with the nucleic acid SYTO61 dye (cells lacking *agr* activity).

using the LSCM 3D package of the Leica SP2 software. The number of sessile cells and the percentage of cells expressing GFP were quantified with light emission intensity using PHLIP and the Matlab toolbox developed by Joao Xavier (www.phlip.org). This software was used to evaluate biofilm structural parameters (biovolume and thickness). For each experiment, five microscopic fields, chosen haphazardly, were analyzed.

The fluorescence loss in photobleaching (FLIP) of intracytoplasmic GFP was used to evaluate if the chains were single elongated cells or separate short rods

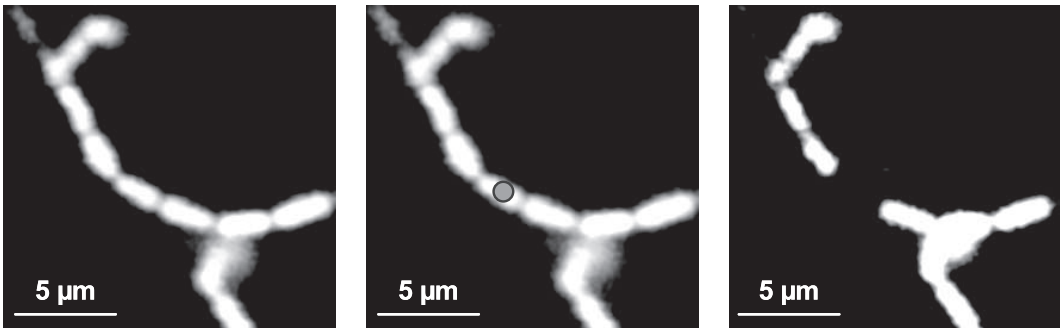

FIG. 2. FLIP of intracytoplasmic GFP within chains. A fluorescent *L. monocytogenes* chain was repeatedly photobleached within a small region (indicated by a gray circle) for ~60 s while the whole chain was continuously imaged. Single elongated cells being photobleached would gradually lose fluorescence due to the lateral movement of mobile GFP into this area. By contrast, the fluorescence in separate short rods near the area being bleached would not be affected.

(59). A fluorescent *L. monocytogenes* chain was repeatedly photobleached for ~60 s within a small region while the whole chain was continuously imaged. Any connected cell in the area of the chain being bleached gradually loses fluorescence due to the lateral movement of mobile GFP into this area. By contrast, the fluorescence in unconnected cells is not affected.

Statistical analysis. A one-way analysis of variance was performed using the SigmaStat, version 3.0.1, software (SPSS Inc.) in order to test the significance of the differences in biovolume or the thickness of biofilms. When the result of the one-way analysis of variance was significant, the Holm-Sidak test ($P < 0.05$) was used to locate significant differences.

RESULTS

A network of knitted chains of *L. monocytogenes* EGD-e were observed only under flow conditions. The sessile growth of *L. monocytogenes* AR009 was monitored under static and flowing conditions using LSCM. Under static conditions, after 2 h of contact with the surface, a few cells were scattered on the surface (Fig. 1A). After 24 h of growth, most of the surface was covered by a monolayer of cells (Fig. 1A). After 48 h of incubation, several layers of cells covered the surface as a uniform biofilm. The 3D reconstruction of the LSCM image stacks confirmed these results of a uniform biofilm that can be described as unorganized multicellular layers of cells covering the surface (Fig. 1A). The structure of the biofilm grown under flowing conditions was different. In fact, after the initial adhesion of *L. monocytogenes* AR009 as single cells, the biofilm developed as a complex structure in which dense, ball-shaped microcolonies separated by poorly colonized zones were observed (16 h) (Fig. 1B). These structures were thicker after 24 and 40 h of incubation (Fig. 1B). Observations under a stronger magnification and 3D analysis evidenced that these microcolonies were surrounded by a network of knitted chains (Fig. 1 and C).

Surprisingly, the morphology of *L. monocytogenes* was affected by the environmental growth conditions; while short rods typical of *L. monocytogenes* morphology were seen under static conditions (Fig. 1A), long chains formed the network of knitted chains under dynamic conditions (Fig. 1B and C). FLIP results confirmed by photobleaching that these structures were chains of short rods and not elongated filamentous cells (Fig. 2). These results pointed to a distinct structure of biofilm that was composed of a network of knitted chains when *L. monocytogenes* was grown under flow conditions.

The influence of the hydrodynamic conditions on the structure of the biofilm also was observed using two structural parameters: biofilm volume (Fig. 3A) and thickness (Fig. 3B). Indeed, the biofilm's volume increased during incubation irrespective of the hydrodynamic conditions. Under dynamic conditions, a significant increase ($P < 0.05$) was observed 24 h after the beginning of the experiment, but the differences were no longer significant after that time. Under static conditions, the increase was significant ($P < 0.05$) at 48 h (Fig. 3A). Interestingly, under dynamic conditions, the biofilm's volume

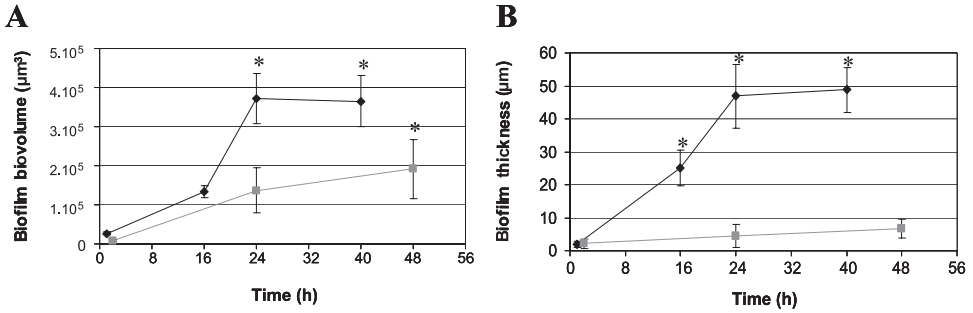

FIG. 3. Biovolume (A) and thickness (B) of *L. monocytogenes* AR009 biofilms in TSB medium at 25°C under static conditions after 2, 24, and 48 h of incubation (square on the gray line) and under flowing conditions after 1, 16, 24, and 48 h of incubation (diamond on the black line). For these quantitative analyses, images obtained by LSCM were analyzed using the PHLIP Matlab routine. The data represent the means and standard deviations from three independent experiments with five measurements for each point. Asterisks indicate statistically significant differences ($P < 0.05$).

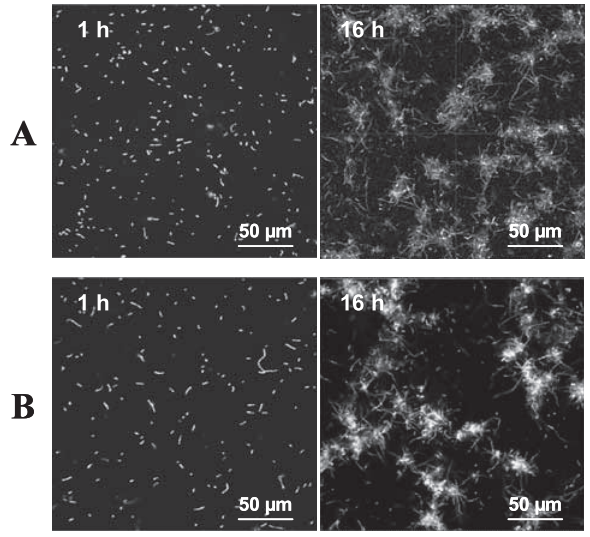

FIG. 4. Scanning confocal micrographs of biofilms formed by *L. monocytogenes* AR009 (A) and *L. monocytogenes* AR011 (Δ*agrA*) (B) in TSB medium at 25°C under flowing conditions after 1 and 16 h of incubation. The images were acquired using LSCM settings with a ×63 objective.

was significantly higher than the volume that was calculated under static conditions from 24 to 48 h ($P < 0.05$) (Fig. 3A). On the other hand, biofilm thickness increased during growth under dynamic conditions ($P < 0.05$), but the differences were not significant under static conditions (Fig. 3B). Furthermore, under dynamic conditions, the biofilm's thickness was significantly increased ($P < 0.05$) after 16, 24, and 40 h of sessile growth (Fig. 3B).

***agr* expression in *L. monocytogenes* biofilms.** We have recently demonstrated that the *agr* system is involved in the onset of *L. monocytogenes* biofilm (48). In order to investigate the expression of the *agr* genes, we used GFP as a reporter. Strain AR009 harbors the reporter plasmid pGID128, in which the promoter region required for *agr*-dependent expression is fused to the *gfp* gene. Under static conditions, irrespective of the length of incubation (2, 24, or 48 h), only a few cells expressing GFP were detected (no more than 1% of the total number of cells expressing *agr* after 48 h) (Fig. 1A). In contrast, during the 40 h of incubation in flowing conditions, *agr* expression increased progressively over time. Indeed, the percentages of cells expressing *agr* were, respectively, 15, 50, 76, and 80% of the total number of cells after 1, 16, 24, and 40 h of growth (Fig. 1B). Most of the GFP fluorescence was observed within the network of knitted chains surrounding the ball-shaped microcolonies, whereas bacteria inside the microcolonies showed very little GFP fluorescence (Fig. 1C).

The *agr* system in biofilm development of *L. monocytogenes*. The role of the *agr* system during biofilm development in flow cells was examined by comparing the behavior of strain AR011, an *agrA* in-frame deletion mutant, to the behavior of AR009. The deletion of *agrA*, the gene coding for the response regulator AgrA, affected the adhesion of *L. monocytogenes* to the surface, as previously described (48) (Fig. 4). The number of adhered cells of strain AR011 (Δ*agrA*) was 3.5-fold lower. However, after 16 h of incubation, the differences between the sessile growth of AR009 and AR011 were not significant (Fig. 4). Moreover, a similar network of knitted chains was observed irrespective of the strain examined. These results confirmed the involvement of the *agr* system during the adhesion of *L. monocytogenes* but probably not during the later stages of biofilm development.

DISCUSSION

The dynamics of *L. monocytogenes* biofilm formation and its regulation still is mostly unknown. The literature related to the biofilm structures of *L. monocytogenes* deals with, in most cases, static experiments using SEM (3, 12, 13, 28, 32, 39, 49). LSCM is a powerful in situ visualization tool for the temporal study of the 3D structures of biofilms (27, 29, 30, 45, 55, 58) and has been used to study the biofilm structure of a variety of microorganisms, such as *Pseudomonas aeruginosa* and *S. aureus* (26, 29). Other studies often mention that the structure of microbial biofilms can vary in response to environmental conditions such as nutrient limitation, flow rate, shear, and pressure (56, 63). In this study, we used LSCM to characterize and compare *L. monocytogenes* biofilms grown under two environmental conditions (growth medium flow or no flow) and to investigate *agr*-dependent gene expression in *L. monocytogenes* biofilms.

Significantly greater biofilm volume and thickness were observed under flowing conditions than under static conditions. Our observations of the biofilm under static conditions showed unorganized 3D structures that were similar to those observed previously (3, 12, 13). In contrast, for the biofilm under flow conditions we described another organization of *L. monocytogenes* EGD-e biofilms that consisted of a network of knitted chains that could structure the microcolonies. The mature biofilms of many species, such as *P. aeruginosa*, that are grown in flow cells display structures that have been described as mushroom-like, with a cohesive polymeric matrix interconnected between water channels (29). These studies indicated that surface-associated motility and biosurfactant production both affect the structure of *P. aeruginosa* biofilms (30, 45). In this study, the newly identified structure that we observed in *L. monocytogenes* EGD-e biofilms could contribute to the 3D structure by interconnecting the ball-shaped microcolonies.

To examine the role of the *L. monocytogenes agr* system during biofilm development and its possible role in the biofilm structure observed in flowing conditions, an *agr* fusion to a GFP reporter was generated. Using LSCM, this construction allowed us to determine both temporal and spatial gene expression patterns throughout biofilm formation. Our findings revealed that *agr* gene expression increased progressively over the incubation period. In terms of spatial expression throughout the stratified biofilm, the *agr* gene activity of *L. monocytogenes* was maximal in cells outside ball-shaped microcolonies. It is intriguing that although the in-frame deletion of *agrA*, which encodes a transcriptional regulator, affected adhesion, no differences were observed after the first step of biofilm development or in biofilm structure (48). *agr*-dependent regulation may be transitory; it may suggest that following adhesion, *L. monocytogenes* undergoes profound gene expression alterations during sessile growth, as has been proposed for other microorganisms (21, 24, 60, 62). In the orthologous *agr*

system of *S. aureus*, the expression of *agr* was patched within cell clusters and oscillated with time (65). Moreover, the role of the *agr* system during *S. aureus* development depends on the hydrodynamic conditions of the experimental setup; under static conditions, the disruption of *agr* expression enhanced biofilm formation (61, 65), while under dynamic conditions it had no influence on biofilm formation (65). In *P. aeruginosa*, *las* and *rhl*, two systems of cell-to-cell signaling, control biofilm formation; the *las* system is involved in early biofilm development, whereas the *rhl* system is implicated in the maturation of the biofilm (15, 50). De Kievit et al. (16), demonstrated by spatial analysis that *lasI* and *rhlI* were maximally expressed in cells located at the substratum and that expression decreased with increasing biofilm height. These authors suggested that the increased accumulation of autoinducers at the substratum resulted in the expression of both of these systems. For *L. monocytogenes*, it is proposed that cells were not enclosed in a matrix and the autoinducers could diffuse away from the cells.

In conclusion, our work has yielded a better understanding of *L. monocytogenes* EGD-e biofilm formation. Our data described, for the first time, the existence of a new structure that consists of a network of knitted chains during the growth of *L. monocytogenes* EGD-e in a flowthrough system. We demonstrate that the model used to grow *L. monocytogenes* biofilms (dynamic flow-cell and static models) deeply affects their structure and the spatiotemporal patterns of gene expression. The *agr*-dependent expression of *L. monocytogenes* in biofilm differed from that of an *S. aureus* orthologous system previously described. Deciphering the mechanisms involved in the development of the network of knitted chains that could structure the sessile growth of *L. monocytogenes* EGD-e is an exciting prospect and will contribute to our better understanding of the ecology of this pathogen.

ACKNOWLEDGMENTS

This work was supported by the Ministère de l'Education Nationale de la Recherche et de la Technologie, the Institut National de la Recherche Agronomique, the Université de Bourgogne, and the PRA *Listeria* program. We thank the local government of the Département de Essonnes for the financial support for a laser-scanning confocal microscope (ASTRE no. A02137).

We thank S. Kathariou for providing the pGF-EM vector.

REFERENCES

1. **Beresford, M. R., P. W. Andrew, and G. Shama.** 2001. *Listeria monocytogenes* adheres to many materials found in food-processing environments. J. Appl. Microbiol. **90:**1000–1005.
2. **Blackman, I. C., and J. F. Frank.** 1996. Growth of *Listeria monocytogenes* as a biofilm an various food-processing surfaces. J. Food Prot. **59:**827–831.
3. **Borucki, M. K., J. D. Peppin, D. White, F. Loge, and D. R. Call.** 2003. Variation in biofilm formation among strains of *Listeria monocytogenes*. Appl. Environ. Microbiol. **69:**7336–7342.
4. **Bower, C. K., J. McGuire, and M. A. Daeschel.** 1996. The adhesion and detachment of bacteria and spores on food-contact surfaces. Trends Food Sci. Technol. **71:**152–157.
5. **Brackett, R. E.** 1992. Shelf stability and safety of fresh produce as influenced by sanitation and disinfection. J. Food Prot. **55:**808–814.
6. **Briandet, R., V. Leriche, B. Carpentier, and M.-N. Bellon-Fontaine.** 1999. Effect of the growth procedure on the surface hydrophobicity of *Listeria monocytogenes* cells and their adhesion to stainless steel. J. Food Prot. **62:**994–998.
7. **Briandet, R., T. Meylheuc, C. Maher, and M.-N. Bellon-Fontaine.** 1999. *Listeria monocytogenes* ScottA: cell surface charge, hydrophobicity, and electron donor and acceptor characteristics under different environmental growth conditions. Appl. Environ. Microbiol. **65:**5328–5333.
8. **Carpentier, B., and O. Cerf.** 1993. Biofilms and their consequences, with particular reference to hygiene in the food industry. J. Appl. Microbiol. **75:**499–511.
9. **Carpentier, B., and D. Chassaing.** 2004. Interactions in biofilms between *Listeria monocytogenes* and resident microorganisms from food industry premises. Int. J. Food Microbiol. **97:**111–122.
10. **Chae, M. S., and H. Schraft.** 2000. Comparative evaluation of adhesion and biofilm formation of different *Listeria monocytogenes* strains. Int. J. Food Microbiol. **62:**103–111.
11. **Challan Belval, S., L. Gal, S. Margiewes, D. Garmyn, P. Piveteau, and J. Guzzo.** 2006. Assessment of the roles of LuxS, *S*-ribosyl homocysteine, and autoinducer 2 in cell attachment during biofilm formation by *Listeria monocytogenes* EGD-e. Appl. Environ. Microbiol. **72:**2644–2650.
12. **Chavant, P., B. Gaillard-Martinie, and M. Hébraud.** 2004. Antimicrobial effects of sanitizers against planktonic and sessile *Listeria monocytogenes* cells according to the growth phase. FEMS Microbiol. Lett. **236:**241–248.
13. **Chavant, P., B. Martinie, T. Meylheuc, M.-N. Bellon-Fontaine, and M. Hebraud.** 2002. *Listeria monocytogenes* LO28: surface physicochemical properties and ability to form biofilms at different temperatures and growth phases. Appl. Environ. Microbiol. **68:**728–737.
14. **Davey, M. E., and G. A. O'Toole.** 2000. Microbial biofilms: from ecology to molecular genetics. Microbiol. Mol. Biol. Rev. **64:**847–867.
15. **Davies, D. G., M. R. Parsek, J. P. Pearson, B. H. Iglewski, J. W. Costerton, and E. P. Greenberg.** 1998. The involvement of cell-to-cell signals in the development of bacterial biofilm. Science **280:**295–298.
16. **De Kievit, T. R., R. Gillis, S. Marx, C. Brown, and B. H. Iglewski.** 2001. Quorum-sensing genes in *Pseudomonas aeruginosa* biofilms: their role and expression patterns. Appl. Environ. Microbiol. **67:**1865–1873.
17. **Donlan, R. M., and J. W. Costerton.** 2002. Biofilms: survival mechanisms of clinically relevant microorganisms. Clin. Microbiol. Rev. **15:**167–193.
18. **Dornseiffen, J. W.** 1998. Residue aspects of disinfectants used in the food industry. Int. Biodeterior. Biodegrad. **41:**309–312.
19. **Farber, J. M., and P. I. Peterkin.** 1991. *Listeria monocytogenes*, a food-borne pathogen. Microbiol. Rev. **55:**476–511.
20. **Frank, J. F., and R. A. Chmielewski.** 1997. Effectiveness of sanitation with quaternary ammonium compound or chlorine on stainless steel and other domestic food-preparation surfaces. J. Food Prot. **60:**43–47.
21. **Gilmore, K. S., P. Srinivas, D. R. Akins, K. L. Hatter, and M. S. Gilmore.** 2003. Growth, development, and gene expression in a persistent *Streptococcus gordonii* biofilm. Infect. Immun. **71:**4759–4766.
22. **Hancock, L. E., and M. Perego.** 2004. The *Enterococcus faecalis fsr* two-component system controls biofilm development through production of gelatinase. J. Bacteriol. **186:**5629–5639.
23. **Harvey, J., K. P. Keenan, and A. Gilmour.** 2007. Assessing biofilm formation by *Listeria monocytogenes* strains. Food Microbiol. **24:**380–392.
24. **Hefford, M. A., S. D'Aoust, T. D. Cyr, J. W. Austin, G. Sanders, E. Kheradpir, and M. L. Kalmokoff.** 2005. Proteomic and microscopic analysis of biofilms formed by *Listeria monocytogenes* 568. Can. J. Microbiol. **51:**197–208.
25. **Holah, J. T., J. H. Taylor, D. J. Dawson, and K. E. Hall.** 2002. Biocide use in the food industry and the disinfectant resistance of persistent strains of *Listeria monocytogenes* and *Escherichia coli*. J. Appl. Microbiol. **92**(Symp. Suppl.)**:**111S–120S.
26. **Jefferson, K. K., D. A. Goldmann, and G. B. Pier.** 2005. Use of confocal microscopy to analyse the rate of vancomycin penetration through *Staphylococcus aureus* biofilms. Antimicrob. Agents Chemother. **49:**2467–2473.
27. **Jones, S. M., J. Yerly, Y. Hu, H. Ceri, and R. Martinuzzi.** 2007. Structure of *Proteus mirabilis* biofilms grown in artificial urine and standard laboratory media. FEMS Microbiol. Lett. **268:**16–21.
28. **Kalmokoff, M. L., J. W. Austin, X. D. Wan, G. Sanders, S. Banerjee, and J. M. Farber.** 2001. Adsorption, attachment and biofilm formation among isolates of *Listeria monocytogenes* using model conditions. J. Appl. Microbiol. **91:**725–734.
29. **Klausen, M., A. Aaes-Jorgensen, S. Molin, and T. Tolker-Nielsen.** 2003. Involvement of bacterial migration in the development of complex multicellular structures in *Pseudomonas aeruginosa* biofilms. Mol. Microbiol. **50:**61–68.
30. **Klausen, M., A. Heydorn, P. Ragas, L. Lambertsen, A. Aaes-Jorgensen, S. Molin, and T. Tolker-Nielsen.** 2003. Biofilm formation by *Pseudomonas aeruginosa* wild type, flagella and type IV pili mutants. Mol. Microbiol. **48:**1511–1524.
31. **Korber, D. R., G. G. Greer, G. M. Wolfaardt, and S. Kohlman.** 2002. Efficacy enhancement of trisodium phosphate against spoilage and pathogenic bacteria in model biofilms and on adipose tissue. J. Food Prot. **65:**627–635.
32. **Krysinski, E. P., L. J. Brown, and T. J. Marchisello.** 1992. Effect of cleaners and sanitizers on *Listeria monocytogenes* attached to product contact surfaces. J. Food Prot. **55:**246–251.
33. **Lemon, K. P., D. E. Higgins, and R. Koler.** 2007. Flagellar motility is critical for *Listeria monocytogenes* biofilm formation. J. Bacteriol. **189:**4418–4424.
34. **Lewis, K.** 2001. Riddle of biofilm resistance. Antimicrob. Agents Chemother. **45:**999–1007.
35. **Li, G., and S. Kathariou.** 2003. An improved cloning vector for construction of gene replacements in *Listeria monocytogenes*. Appl. Environ. Microbiol. **69:**3020–3023.
36. **Lundén, J. M., T. J. Autio, and H. J. Korkeala.** 2002. Transfer of persistent

Listeria monocytogenes contamination between food-processing plants associated with a dicing machine. J. Food Prot. **65:**1129–1133.
37. **Lundén, J. M., M. K. Miettinen, T. J. Autio, and H. J. Korkeala.** 2000. Persistent *Listeria monocytogenes* strains show enhanced adherence to food contact surface after short contact times. J. Food Prot. **63:**1204–1207.
38. **Mah, T.-F. C., and G. A. O'Toole.** 2001. Mechanisms of biofilm resistance to antimicrobial agents. Trends Microbiol. **9:**34–38.
39. **Marsh, E. J., H. Luo, and H. Wang.** 2003. A three-tiered approach to differentiate *Listeria monocytogenes* biofilm-forming abilities. FEMS Microbiol. Lett. **228:**203–210.
40. **Meyer, B.** 2003. Approaches to prevention, removal and killing of biofilms. Int. Biodeterior. Biodegrad. **51:**249–253.
41. **Monk, I. R., G. M. Cook, B. C. Monk, and P. J. Bremer.** 2004. Morphotypic conversion in *Listeria monocytogenes* biofilm formation: biological significance of rough colony isolates. Appl. Environ. Microbiol. **70:**6686–6694.
42. **Murray, E. G. D., R. A. Webb, and M. B. R. Swann.** 1926. A disease of rabbits characterised by a large mononuclear leucocytosis, caused by a hitherto undescribed bacillus *Bacterium monocytogenes*. J. Pathol. Bacteriol. **29:**407–439.
43. **Norwood, D. E., and A. Gilmour.** 1999. Adherence of *Listeria monocytogenes* strains to stainless steel coupons. J. Appl. Microbiol. **86:**576–582.
44. **O'Toole, G., H. B. Kaplan, and R. Kolter.** 2000. Biofilm formation as microbial development. Annu. Rev. Microbiol. **54:**49–79.
45. **Pamp, S. J., and T. Tolker-Nielsen.** 2007. Multiple roles of biosurfactants in structural biofilm development by *Pseudomonas aeruginosa*. J. Bacteriol. **189:**2531–2539.
46. **Pan, Y., F. Breidt, Jr., and S. Kathariou.** 2006. Resistance of *Listeria monocytogenes* biofilms to sanitizing agents in a simulated food processing environment. Appl. Environ. Microbiol. **72:**7711–7717.
47. **Ren, T. J., and J. F. Frank.** 1993. Susceptibility of starved planktonic and biofilm *Listeria monocytogenes* to quaternary ammonium sanitizer as determined by direct viable and agar plate counts. J. Food Prot. **56:**573–576.
48. **Rieu, A., S. Weidmann, D. Garmyn, P. Piveteau, and J. Guzzo.** 2007. *agr* system of *Listeria monocytogenes* EGD-e: role in adherence and differential expression pattern. Appl. Environ. Microbiol. **73:**6125–6133.
49. **Sasahara, K. C., and E. A. Zottola.** 1993. Biofilm formation by *Listeria monocytogenes* utilizes a primary colonizing microorganism in flowing systems. J. Food Prot. **56:**1022–1028.
50. **Sauer, K., A. K. Camper, G. D. Ehrlich, J. W. Costerton, and D. G. Davies.** 2002. *Pseudomonas aeruginosa* displays multiple phenotypes during development as a biofilm. J. Bacteriol. **184:**1140–1154.
51. **Sela, S., S. Frank, E. Belausov, and R. Pinto.** 2006. A mutation in the *luxS* gene influences *Listeria monocytogenes* biofilm formation. Appl. Environ. Microbiol. **72:**5653–5658.
52. **Smoot, L. M., and M. D. Pierson.** 1998. Effect of environmental stress on the ability of *Listeria monocytogenes* ScottA to attach to food contact surfaces. J. Food Prot. **61:**1293–1298.
53. **Smoot, L. M., and M. D. Pierson.** 1998. Influence of environmental stress on the kinetics and strength of attachment of *Listeria monocytogenes* ScottA to Buna-N rubber and stainless steel. J. Food Prot. **61:**1286–1292.
54. **Somers, E. B., and A. C. Wong.** 2004. Efficacy of two cleaning and sanitizing combinations on *Listeria monocytogenes* biofilms formed at low temperature on a variety of materials in the presence of ready-to-eat meat residue. J. Food Prot. **67:**2218–2229.
55. **Sternberg, C., B. B. Christensen, T. Johansen, A. Toftgaard Nielsen, J. B. Andersen, M. Givskov, and S. Molin.** 1999. Distribution of bacterial growth activity in flow-chamber biofilms. Appl. Environ. Microbiol. **65:**4108–4117.
56. **Stickler, D.** 1999. Biofilms. Curr. Opin. Microbiol. **2:**270–275.
57. **Sturme, M. H. J., J. Nakayama, D. Molenaar, Y. Murakami, R. Kunugi, T. Fujii, E. E. Vaughan, M. Kleerebezem, and W. M. de Vos.** 2005. An *agr*-like two-component regulatory system in *Lactobacillus plantarum* is involved in production of a novel cyclic peptide and regulation of adherence. J. Bacteriol. **187:**5224–5235.
58. **Tolker-Nielsen, T., U. C. Brinch, P. C. Ragas, J. B. Andersen, C. S. Jacobsen, and S. Molin.** 2000. Development and dynamics of *Pseudomonas* sp. biofilms. J. Bacteriol. **182:**6482–6489.
59. **van Drogen, F., and M. Peter.** 2004. Revealing protein dynamics by photobleaching techniques. Methods Mol. Biol. **284:**287–306.
60. **Vilain, S., P. Cosette, M. Hubert, C. Lange, G.-A. Junter, and T. Jouenne.** 2004. Comparative proteomic analysis of planktonic and immobilized *Pseudomonas aeruginosa* cells: a multivariate statistical approach. Anal. Biochem. **329:**120–130.
61. **Vuong, C., H. L. Saenz, F. Gotz, and M. Otto.** 2000. Impact of the *agr* quorum-sensing system on adherence to polystyrene in *Staphylococcus aureus*. J. Infect. Dis. **182:**1688–1693.
62. **Whiteley, M., M. G. Bangera, R. E. Bumgarner, M. R. Parsek, G. M. Teitzel, S. Lory, and E. P. Greenberg.** 2001. Gene expression in *Pseudomonas aeruginosa* biofilms. Nature **413:**860–864.
63. **Wimpenny, J., W. Manz, and U. Szewzyk.** 2000. Heterogeneity in biofilms. FEMS Microbiol. Rev. **24:**661–671.
64. **Xu, K. D., G. A. McFeters, and P. S. Stewart.** 2000. Biofilm resistance to antimicrobial agents. Microbiology **146:**547–549.
65. **Yarwood, J. M., D. J. Bartels, E. M. Volper, and E. P. Greenberg.** 2004. Quorum sensing in *Staphylococcus aureus* biofilms. J. Bacteriol. **186:**1838–1850.